

**IEEE Transactions on Nuclear Science, Vol. NS-28. No. 3. June 1981**  
**FERMILAB ENERGY DOUBLER BEAM POSITION DETECTOR**  
**R. E. Shafer, R. C. Webber, and T. H. Nicol**  
**Fermi National Accelerator Laboratory\***  
**P.O. Box 500**  
**Batavia, Illinois 60510**

### **Summary**

This paper describes the design and performance of the beam position detector being installed in the Fermilab superconducting Energy Doubler accelerator. The detector is a stripline pickup designed to operate at 4 degrees Kelvin and with beam intensities ranging from  $10^8$  to  $10^{11}$  protons per RF bucket at 53 MHz. The detector design, signal amplitude, positional sensitivity, directivity, and longitudinal impedance are presented.

### **Introduction**

In order to adequately control the steering of the beam in the Energy Doubler, position detectors are needed every 30 m around the entire 6.28 km circumference. These detectors will be located at every quadrupole to monitor beam position in the quadrupole focusing plane. There will be roughly 220 detectors in all, approximately 110 monitoring the vertical position, and 110 the horizontal. Among special considerations bearing on the design were the requirements that they operate at liquid helium temperatures, and that the accelerator would eventually have simultaneous counter-rotating proton and anti-proton beams.

### **Design**

A cross sectional view of the detector is shown in Figure 1. Each detector has two 18 cm long copper electrodes in a 10.2 cm diameter stainless steel pipe. Each electrode is bent to a 3.5 cm radius of curvature, and subtends 110 degrees of arc for a centered beam. The available

aperture is about 7 cm, the same as the accelerator beam pipe. The arc length and the spacing from the wall of the stainless steel pipe were selected to provide a uniform position response (including lack of sensitivity to motion in the orthogonal plane), while rigorously maintaining a 50 ohm transmission line impedance. Both electrodes are supported by two small 0.5 cm diameter G-10 standoffs at each end, in order that the transmission line propagation velocity be as close to  $c$  as possible. At each end of both electrodes, a

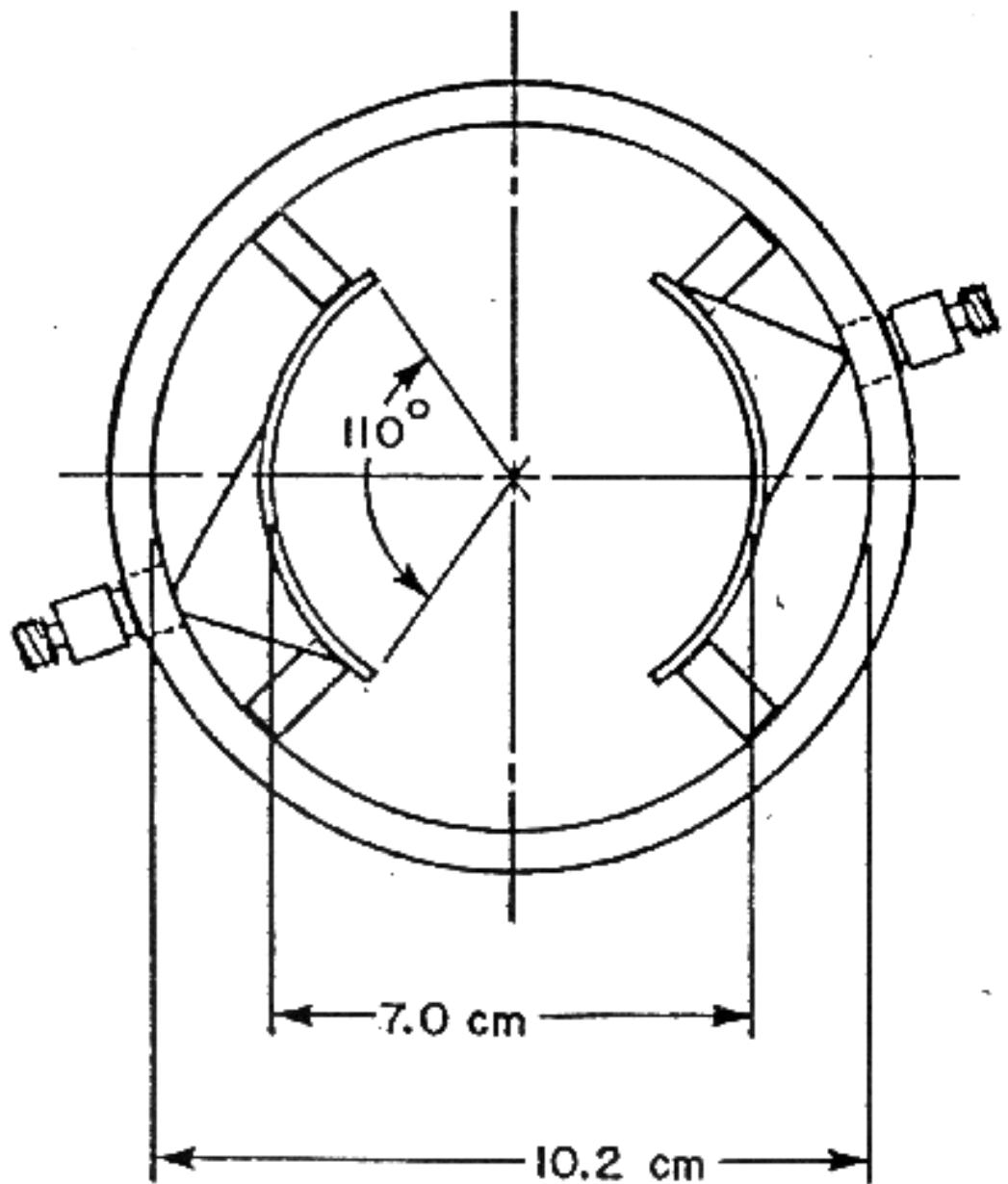


**FIGURE 1. Cross sectional view of the stripline position detector.**

ceramic-sealed SMA style coaxial feedthrough connector is installed. The feedthrough connectors had to be placed off-center due to interference with cryogenic plumbing in the magnet. A triangular taper of thin copper foil connects the pickup electrode to the feedthrough connector to reduce the inductance of the connection. In addition, the inner diameter of the end caps is tapered at a 45 degree angle to provide additional impedance matching. The overall length of the detector, including end caps, is 23 cm. In selecting materials for the the detector, special consideration was given to the fact that it would be operating at 4 degrees Kelvin, and that there would be thermal stresses due to differential expansion and contraction during warmup and cooldown of the accelerator. The detector is installed inside the quadrupole cryostat and is rigidly welded to the quadrupole coil mechanical support, in order to insure relative alignment to  $\pm 0.05$  cm. Each detector is cabled to the outer cryostat wall with four 50 cm long RG-178 coaxial cables, which attach to hermetically sealed coaxial feedthrough connectors. The estimated heat leak along each cable is 150 mW.

In normal operation, the downstream port of each electrode will be terminated in 50 ohms at the outer cryostat feedthrough. Although back terminations are not mandatory from the standpoint of signal amplitude at the upstream ports, they do reduce the noise power as seen by the electronics, as back terminations absorb rather than reflect noise power. Furthermore, the back termination will reduce any standing waves caused by impedance mismatches. The termination technique used here differs from an earlier design electrostatic position detector<sup>1</sup> in several ways. The back terminations are now at room temperature and accessible for maintenance. The problem of finding a terminating resistance which is 50 ohms at liquid helium temperatures no longer exists. In the earlier design, the back termination absorbed half the signal power as well, reducing the already small signals at low beam intensities required to tune up a superconducting accelerator, and adding a significant heat load to the cryogenic system at high beam intensities. The total power output per electrode during CW operation with a 1 nsec RMS proton bunch width is estimated to be 2.8  $\mu$  W at  $10^8$  protons/bunch, and 2.8  $\mu$  W at  $10^{11}$  protons/bunch.

Each detector is connected to the processing electronics by foam-dielectric RG-8 type cable, ranging in length from 50 m to 200 m. The cables need to be phase matched to  $\pm 20$  degrees in phase at 53 MHz. Eventually, when the accelerator has a counter-rotating anti-proton beam, coaxial switches will be installed at the detectors to select the proper pair of ports.

### Performance

The approximate response of the detector to the passage of the beam may be estimated in the following Banner. Assume a centered proton bunch containing N protons of unit charge e in a longitudinal Gaussian shaped pulse of RMS length sigma (in units of time). The instantaneous current is

$$I(t) = \frac{eN}{\sqrt{2\pi}\sigma} \exp \left[ \frac{-t^2}{2\sigma^2} \right] \quad (1)$$

The wall image current is equal in amplitude and opposite polarity. As this proton bunch approaches the upstream end of the electrode, a fraction F of the wall current is induced on the Inside surface of the electrode.  $2\pi F$  is approximately the azimuthal angle subtended by the electrode. Two positive polarity signals are induced on the outside surface of the electrode, each of amplitude  $F/2$ . One signal flows out the upstream port, and the other along the outside surface of the electrode. This latter signal has the same propagation velocity as the beam, and arrives at the downstream end of the electrode simultaneous with the proton beam. Two additional pulses are induced by the beam at the downstream end of the electrode, one flowing out the downstream port, which is cancelled by the signal flowing on the outside surface of the

electrode, and the other signal flowing upstream on" the outside surface of the electrode and out the upstream port. The signal seen at the upstream port is then

$$V(t) = \frac{ZF}{2} \{I(t+t_0) - I(t-t_0)\} \quad (2)$$

where  $Z$  is the characteristic impedance of the electrode and cable, and  $t_0$  the propagation delay along the electrode. If this bipolar doublet pulse is periodic with period  $T = 2\pi/\omega$  where  $\omega$  is the fundamental angular RF frequency, the peak voltage of the  $m^{\text{th}}$  harmonic of the RF frequency is

$$V_m = \frac{\omega}{\pi} \int_{-T/2}^{T/2} V(t) \sin(m\omega t) dt \quad (3)$$

The peak voltages for the first few harmonics are plotted in Figure 2 vs the RMS bunch width  $\sigma$ , for  $N = 10^{10}$  protons/bunch,  $F = 0.3$ ,  $Z = 50$  ohms,  $\omega/2\pi = 53$  MHz, and  $t_0 = 0.61$  nsec. We have installed a detector in the Main Ring, and the observed voltages for  $m=1$  are in agreement with the calculated value when the cable attenuation is taken into account. Note that all harmonics are dependent on the proton bunch width  $\sigma$ . In the Main Ring during the acceleration cycle, the  $m=1$  amplitude normally increases by about 15% at the end of the injection cycle due to the increased RF voltage applied during acceleration, causing the proton bunch length to shrink.

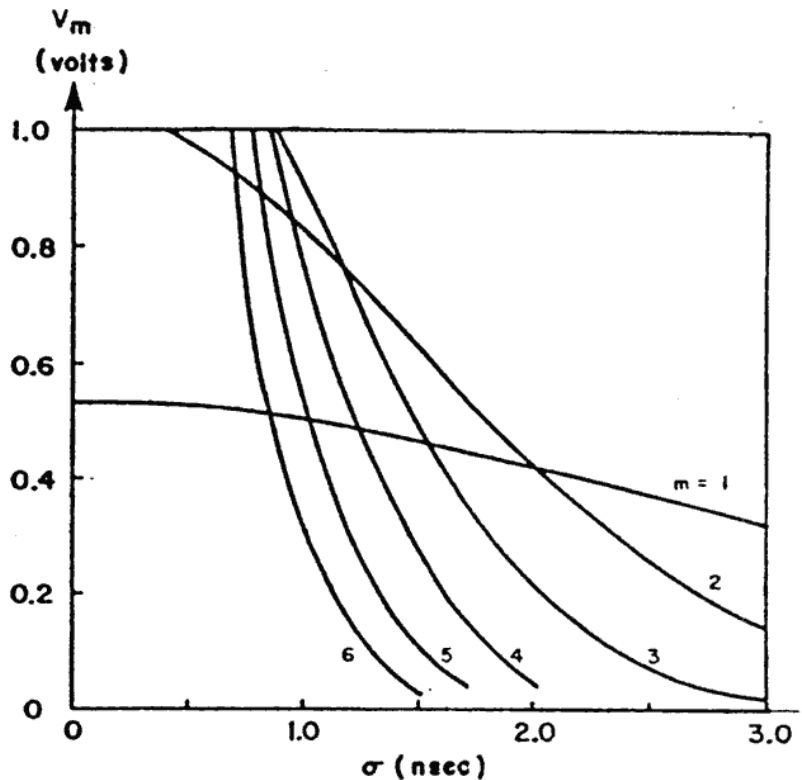


FIGURE 2. Peak voltage output for pickup electrode signal into 50 ohms, vs RMS proton bunch width, for various harmonics of 53 MHz, at  $10^{10}$  protons/bunch.

The beam position is determined by measuring the relative amplitude of the signals from the two posing electrodes. This is calculable assuming the electrostatic equivalent model is adequate, and calculating the total charge induced on each electrode for various locations of a line charge in the aperture. The choice of 110 degrees for the azimuthal arc length of the electrodes appeared to give the best combination of signal amplitude, linearity to beam displacement in the plane connecting the two electrodes, and insensitivity to beam displacement in the orthogonal plane. Measurements of the actual sensitivity using a pulsed .06 cm diameter wire are shown in Figure 3. Near the center, the sensitivity is

$$S = \frac{20}{x} \log (A/B) = 6.7 \text{db/cm} \quad (4)$$

where A and B are the induced signal amplitudes on the electrodes. The electronic technique used to detect this relative amplitude is amplitude-to-phase conversion, described elsewhere in this Proceedings.<sup>2</sup> This technique was considered necessary in order to rapidly measure the beam position (nominally a 200 nsec sampling time is adequate) over a 1000:1 range in beam intensities. Repetitive sampling of a 200 nsec segment of beam in the Main Ring at  $10^{10}$  protons/bunch shows the RMS resolution of the system to be about 30 microns, as can be seen in Figure 4. The absolute resolution at all intensities is expected to be better than 500 microns.

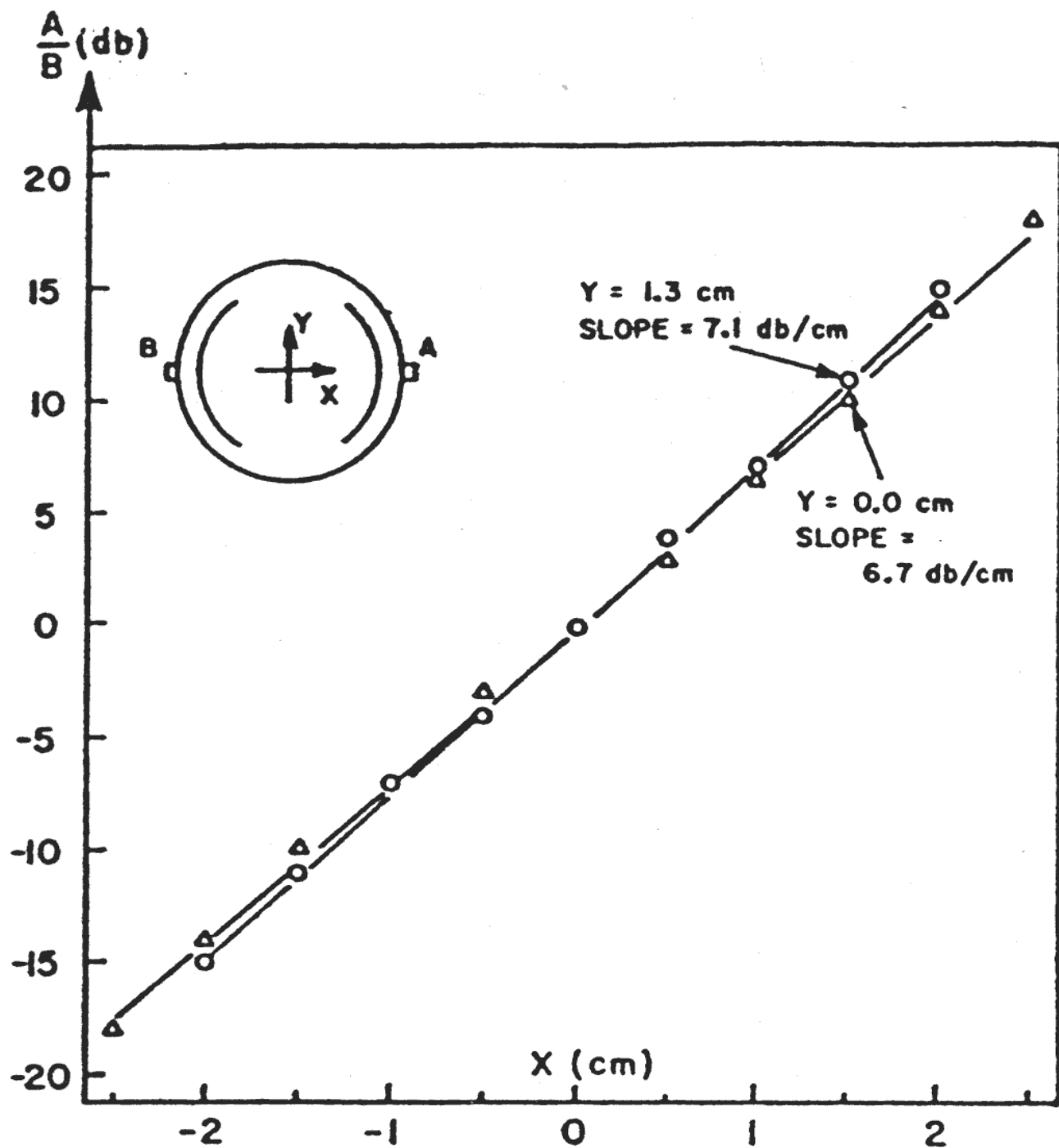


FIGURE 3. Position sensitivity of beam position detector. Measurements of relative A and B signal amplitudes as a function of test wire position.

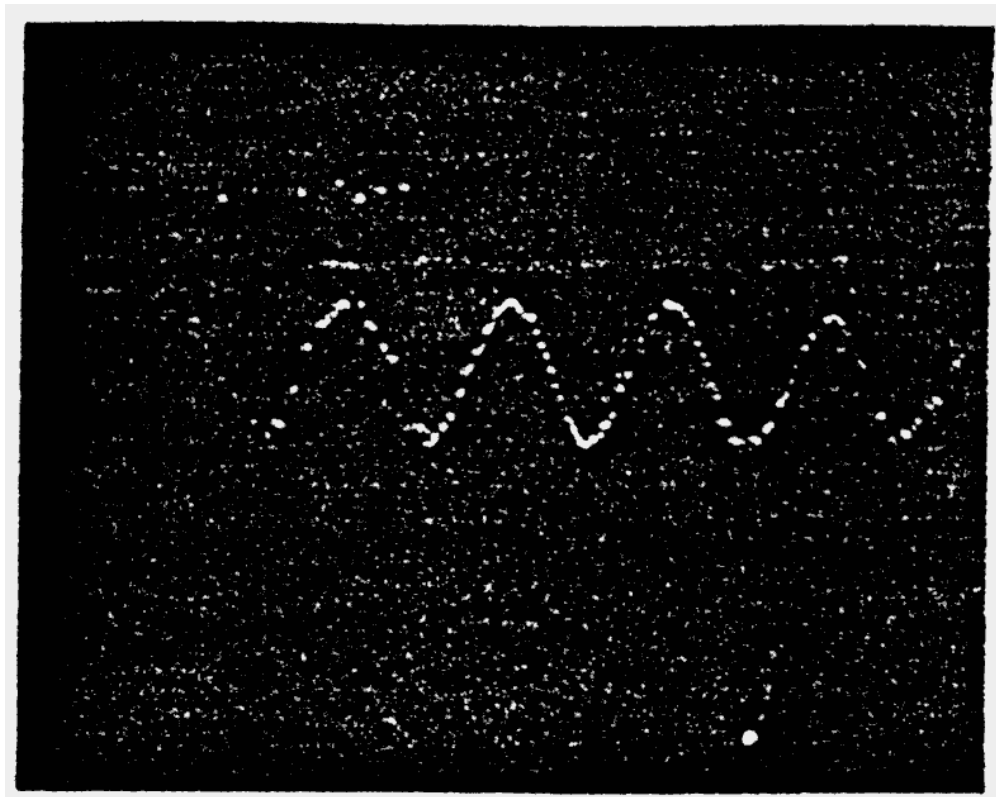


FIGURE 4. Horizontal beam position vs time for beam injected into Main Ring. Vertical axis is 500 microns per major division. Horizontal . axis is 1 msec per major division. The synchrotron oscillation frequency is about 600 Hz. The RMS resolution is about 30 microns.

Measurements on production units also include both a VSWR and directivity measurement at 53 MHz. Typical VSWR, including the effect of the RG-178 cables and connectors is about 1.04. Directivity is about 22 db (relative signal amplitude ratio from the upstream and downstream ports). A good directional coupler should yield a directivity exceeding 30 db. The low value obtained here is due in part to the large coupling capacitance of the two electrodes, and to impedance discontinuities at the various connections.

### **Longitudinal Impedance**

The effect of the detector on the beam is calculated in the following way. The voltage output of the detector, and hence the power dissipation in the terminating resistor at an angular frequency  $\omega$ , is calculated assuming a sinusoidal longitudinal spatial dependence of the proton beam charge density in equation (1). The source of this power may be considered as representing the beam current flowing through a resistance which is frequency dependent. The reactive component of this longitudinal impedance may be calculated by dispersion relations.<sup>3</sup> The resultant impedance for a single detector (2 electrodes) as seen by the beam current is:<sup>4</sup>

$$Z_L(\omega) = 2ZF^2 (\sin^2(\omega t_0) + j\sin(\omega t_0)\cos(\omega t_0)) \quad (5)$$

The reactive impedance is inductive up to about 420 MHz, capacitive from 420 to 840 MHz, and inductive again above 840 MHz. For the Energy Doubler, this calculation predicts an approximate low frequency  $Z/n = +j 0.35$  ohms for 216 detectors (this is the reactive impedance seen by the beam at the revolution frequency). Measurements using a network analyzer at frequencies up to 1.3 GHz are consistent with this estimate, and show no resonances attributable to the detector cavity.

### Acknowledgments

The authors would like to thank Q. Kerns and F. Mills for illuminating discussions on beam detectors, and E. Faught for assistance in making the measurements.

### References

1. E.F. Higgins and T.H. Nicol, IEEE Trans. Nucl. Sci. NS-26, #3 page 3426 (June 1979).
2. S. P. Jachim, R. C. Webber, and R.E. Shafer, this Proceedings.
3. H.W. Bode, "Network Analysis and Feedback Amplifier Design", Van Norstrand (1945); see especially chapter 14 and the table on page 335.
4. R. E. Shafer, Fermilab internal report #UPC-133, 7/15/80, unpublished.

\*Operated by Universities Research Association, Inc. under contract with the U.S. Department of Energy.